Carbohydrate Research, 48 (1976) 105–124

SUBSITE MAPPING OF ENZYMES: COLLECTING AND PROCESSING EXPERIMENTAL DATA—A CASE STUDY OF AN AMYLASE–MALTO-OLIGOSACCHARIDE SYSTEM

JOHN A. THOMA AND JIMMY D. ALLEN
Department of Chemistry, University of Arkansas, Fayetteville, Arkansas 72701 (U. S. A.)
(Received June 25th, 1975; accepted for publication in revised form, December 15th, 1975)

ABSTRACT

Two research groups have independently developed the theory and experimental methodology for quantitatively assessing substrate monomer–subsite binding-energies for depolymerases. When the two approaches are applied to the same enzyme–substrate system they yield surprisingly divergent results. This paper outlines the application of the two approaches to an amylase–maltooligosaccharide system and points out the more important areas of disagreement. We show that by proper data-management, the conflicts between the two laboratories are basically resolved. The complexities of the subsite model demand extensive data-gathering and exacting data-processing and verification that the computed model-parameters can faithfully reproduce the experimental data.

DISCUSSION

For several years, the enzymic properties of proteases[1–7], nucleases[8–11], and carbohydrases[12–27] have been rationalized on the basis of a subsite model. According to this model, the binding region of the enzyme is visualized as a tandem array of modules (subsites) that interact with the monomer units of the substrate (see Fig. 1). More often, monomer–subsite interactions release energy, but ocassionally unfavorable steric contacts between the monomer and subsites result in a positive free-energy of interaction[17]. According to the model, oligomers can bind to the enzyme and may occupy the whole binding-region or only parts of it. Binding of a particular substrate in different sets of subsites gives rise to a group of complexes called positional isomers. Two general classes of positional isomers exist: productive complexes in which the bound substrate exposes a susceptible bond to the catalytic amino acids and suffers bond cleavage (as in binding mode IX, 4 of Fig. 1), and nonproductive complexes in which the bound substrate does not expose a susceptible bond to the catalytic amino acids and does not suffer bond cleavage (as in binding mode III,4 of Fig. 1).

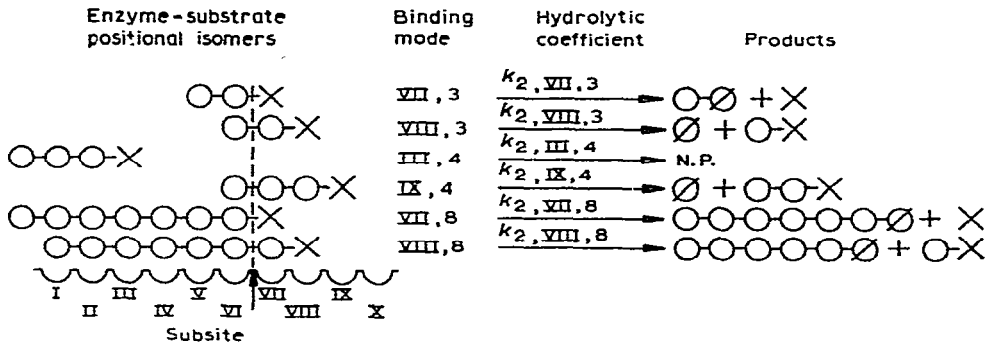

Fig. 1. Some positional isomers of *B. amyloliquefaciens* amyiase: U, subsite on the enzyme; ↑, position of the catalytic site; O, D-glucopyranoside residue; ∅, reducing D-glucopyranose residue; ×, reducing radiolabeled D-glucopyranose residue; ——, α-(1→4) bond. The term $k_{2,i,n}$ is a microscopic, hydrolytic rate-coefficient for chain length n in binding mode i. The binding mode is designated by a Roman number indicating the subsite holding the reducing residue and an Arabic number indicating the chain length of the substrate. N. P. indicates that the binding mode is nonproductive. The dotted line represents the point of bond cleavage.

Each of these positional isomers is characterized by a microscopic equilibrium constant, K', defined by the relationship*

$$\Delta\tilde{G}_{\text{total}} = \sum_i \Delta\tilde{G} + 2400 = -RT \ln K', \qquad (1)$$

where $\Sigma\Delta\tilde{G}_i$ is the sum of the free energies of binding of the filled subsites and 2400 calories.mole^{-1} is the cratic free-energy of mixing[28]. The sum of these microscopic binding-constants for all positional isomers of a given substrate is the macroscopic binding-constant for that substrate. The inverse of the apparent Michaelis parameter, $\tilde{K}_m$, approaches this macroscopic binding-constant as the rate of hydrolysis of bound substrate to the rate of dissociation approaches zero. When this ratio is significantly greater than zero, a correction factor must be applied to convert Michaelis constants to equilibrium constants.

The maximum velocity for the hydrolysis of a given substrate is expressed as:

$$\tilde{V} \frac{\sum_i k_{2,i}\,[\text{productive positional isomers}]}{\sum_i [\text{productive positional isomers} + \text{nonproductive positional isomers}]}, \qquad (2)$$

where i indexes the binding mode (see Fig. 1) and $k_{2,i}$ is the microscopic hydrolytic-coefficient for that binding mode. The concentration of any positional isomer indexed by i can be calculated, given the substrate and enzyme concentrations, and the appropriate microscopic constant defined by Eq. *1*.

The bond-cleavage frequencies for any substrate depend upon the relative concentrations of its positional isomers (or its microscopic association-constants)

*A complete listing of symbols is given at the end of the paper.

and the relative rates of hydrolysis of its positional isomers (or its microscopic hydrolytic-coefficients). For example, consider the breakdown of two end-labeled trisaccharide–amylase complexes, binding modes VII,3 and VIII,3 in Fig. 1. The yield of unlabeled maltose (○–⌀) and labeled D-glucose (×) from the trisaccharide depends on the hydrolytic coefficient $k_{2,\mathrm{VII},3}$ and the concentration of binding mode VII,3, whereas the yield of unlabeled D-glucose (⌀) and labeled maltose (○–×) depends on the hydrolytic coefficient $k_{2,\mathrm{VIII},3}$ and concentration of binding mode VIII,3. The bond-cleavage frequency for the trisaccharide is related to the product ratios of × and ○–× for these two positional isomers by

$$\frac{[\times]}{[\bigcirc\!-\!\times]} = \frac{k_{2,\mathrm{VII},3}\,[\text{binding mode VII,3}]}{k_{2,\mathrm{VIII},3}\,[\text{binding mode VIII,3}]}. \tag{3}$$

As already noted, the concentration of binding mode VII,3 and binding mode VIII,3 of Eq. *3* may be calculated, given the substrate and enzyme concentrations and the microscopic constants in Eq. *1*.

From the foregoing discussion and Eqs. *1–3*, it may be seen that $\tilde{K}_m$, $\tilde{V}$, and bond-cleavage frequency are directly related to the free energy released in the process of monomer–subsite interactions. To verify this model, based on subsite–monomer interactions, it is necessary to devise general procedures for assessing the individual subsite-energies ($\Delta\tilde{G}_i$) from the experimentally measurable parameters, $\tilde{K}_m$, $\tilde{V}$, and bond-cleavage frequencies. It is then necessary to show that these values of $\Delta\tilde{G}_i$ correctly predict $\tilde{K}_m$, $\tilde{V}$, and bond-cleavage frequencies as a function of chain length. The determination of the number of subsites and their binding affinity for monomer units of the substrate is termed subsite mapping.

Hiromi and coworkers[19–25] and Thoma and coworkers[17,18] have independently developed methods for subsite mapping and have applied the techniques to an amylase–malto-oligosaccharide system. The two research groups have divergent opinions about the type of experimental data required to assess the number of subsites, the method for processing the data to evaluate the subsite–monomer interaction energies, the interpretation of their data, and the assumptions of the model. This paper describes the approaches to subsite mapping employed by the two laboratories, discusses their relative merits and pitfalls, and rationalizes some of the divergent positions.

Synopsis of theoretical treatments. — Detailed theoretical developments of the subsite model and a discussion of the assumptions underlying the model may be found elsewhere[18–20]. In this section, only the equations most valuable for subsite mapping are set forth.

The generalized Michaelis scheme describing binding and degradation of a polymeric substrate is

$$\mathrm{E}+\mathrm{A}_n \underset{k_{-1,i,n}}{\overset{k_{1,i,n}}{\rightleftharpoons}} \mathrm{EA}_{i,n} \xrightarrow{k_{2,i,n}} \mathrm{E}+\mathrm{P}_{i,m}, \tag{4}$$

where i indexes the binding mode, A_n is a substrate of chain length n, $\mathrm{P}_{i,m}$ is a product

of chain length m, E represents enzyme, and k_2 is the microscopic hydrolytic-coefficient for the complex.

A steady-state analysis of Eq. *4* reveals that the important relationships between measured constants and microscopic binding-constants that are directly related to ΔG_i by Eq. *1* are:

$$\frac{1}{\tilde{K}_{m,n}} = \sum_i 1/K_{i,n} = \sum_i K'_{i,n}, \tag{5}$$

$$\frac{\tilde{V}_n}{[E_0]} = \frac{\sum_i k_{2,i,n}/K_{i,n}}{\sum_i 1/K_{i,n}}, \tag{6}$$

and

$$\tilde{v}_{0,n} = \frac{\tilde{V}_n}{\tilde{K}_{m,n}[E_0]} = \sum_i k_{2,i,n}/K_{i,n}, \tag{7}$$

where $\tilde{K}_{m,n}$ and $\tilde{V}_n$ are measured Michaelis constants and $\tilde{v}_{0,n}$ is the first-order rate constant for enzymic hydrolysis at low concentration of substrate ($A \ll \tilde{K}_m$). $K_{i,n}$ approximates a microscopic dissociation-constant and has the form $(k_{-1,i,n}+k_{2,i,n})/k_{1,i,n}$; $K'_{i,n}$ is the corresponding association-constant. The term $\tilde{v}_{0,n}$ contains only terms for productive complexes, as noted previously by Hanson[29].

The other measurable function that yields valuable information about subsite binding-energies is the bond-cleavage frequency of a substrate. The bond-cleavage ratio for a pair of adjacent bonds is:

$$\frac{[\dot{P}_{i,m}]}{[\dot{P}_{i+1,m+1}]} = \frac{k_{2,i,n}/K_{i,n}}{k_{2,i+1,n}/K_{i+1,n}}, \tag{8}$$

where $[\dot{P}] = d[P]/dt$. As $k_{2,i,n} = 0$ for nonproductive complexes, it may be seen that both bond-cleavage frequency (Eq. *8*) and $\tilde{v}_0$ (Eq. *7*) provide information only about productive complexes. On the other hand it may be seen that $\tilde{K}_m$ (Eq. *5*) and $\tilde{V}$ (Eq. *6*) provide information about both productive and nonproductive complexes. Consequently Eqs. *5*, *6*, and *8* must all be used to generate a complete subsite map. Eqs. *5* and *6* are inadequate for this purpose.

Processing of data. — The crux of the subsite-mapping problem is to devise procedures to determine the number of subsites, to locate the position of the catalytic site, and to estimate the free-energy change accompanying monomer binding at each subsite. The chain-length dependence of $\tilde{K}_m$, $\tilde{V}$, and bond-cleavage frequencies are all required data for generating the subsite map. The merit of this subsite map will depend on its ability to account for the behavior of the enzyme toward substrates of various chain-lengths.

Hiromi's group[19–25] and our group[17,18] have independently devised methods for subsite mapping. The two groups collect different but overlapping types of data

TABLE I

EXPERIMENTAL PARAMETERS FOR THREE STRAINS OF *Bacillus amyloliquefaciens* AMYLASE[a]

Chain length	$\tilde{K}_m$ or $\tilde{K}_I$ (M)			$\tilde{V}$ (*relative*)			$\tilde{v}_0$	
	BLA-D[b]	*BLA-F*[b]	*BLA-N*[c]	*BLA-D*[b]	*BLA-F*[b]	*BLA-N*[c]	*BLA-D*[b]	*BLA-F*[b]
1			6.0×10^{-1}					
2			2.2×10^{-2}				5.0×10^{-1}	8.7×10^{-1}
3	1.7×10^{-1}	1.3×10^{-1}	1.9×10^{-2}	1.0	1.0	1.0	5.3×10	5.3×10
4	3.3×10^{-2}	8.7×10^{-2}	1.7×10^{-2}	5.7	4.3	8.3	6.5×10^{2}	4.7×10^{2}
5	3.5×10^{-2}	6.6×10^{-2}	1.9×10^{-2}	1.6×10	1.6×10	2.6×10	2.8×10^{3}	8.4×10^{3}
6	1.6×10^{-2}	3.6×10^{-2}	9.9×10^{-3}	1.6×10^{2}	3.6×10^{2}	1.4×10^{2}	5.5×10^{4}	6.9×10^{4}
7	1.3×10^{-2}	2.1×10^{-2}	5.2×10^{-3}	3.8×10^{2}	6.1×10^{2}	1.0×10^{3}	7.4×10^{5}	5.1×10^{5}
8	3.8×10^{-3}		1.5×10^{-3}	3.6×10^{3}		1.7×10^{3}	3.2×10^{6}	3.9×10^{6}
9			8.8×10^{-4}			4.2×10^{3}		
10			5.6×10^{-4}			4.2×10^{3}		
11			4.9×10^{-4}			4.2×10^{3}		
12			8.6×10^{-4}			4.2×10^{3}		
12.6	1.5×10^{-3}	1.9×10^{-3}		2.5×10^{3}	1.7×10			

[a]See text for explanation of notation. [b]Iwasa *et al.*[23]. [c]Thoma *et al.*[18].

and process and interpret them differently. As both research groups have investigated a bacterial amylase–malto-oligosaccharide system, it is informative to compare the data, techniques, and interpretations. Both groups have investigated the substrate chain-length dependence of $\tilde{K}_m$ and $\tilde{V}$ for three different strains of *Bacillus amyloliquefaciens* amylase* but, in addition, our group has used bond-cleavage frequency analysis as an integral part of the technique. The data are summarized in Table I.

Evaluation of the number of subsites and position of the catalytic site. — An accurate measure of the number of subsites and the location of the catalytic site in the binding region is the critical first step in subsite mapping. Thoma and coworkers[17] used the chain-length dependence of bond-cleavage frequencies and Eq. *8* to determine simultaneously the number of subsites and to position the catalytic site. Eq. *8* can be rearranged and combined with Eq. *1* to give

$$RT \ln \frac{[\dot{P}_{i,m}]}{[\dot{P}_{i+1,m+1}]} = \Delta G_{i+1} - \Delta G_{i-n+1} + RT \ln \frac{k_{2,i,n}}{k_{2,i+1,n}}, \qquad (9)$$

where i is the index of the subsite occupied by the "reducing" monomer unit of a substrate in binding mode i. To obtain a first approximation of a subsite map, the contribution of the kinetic ratio, $k_{2,i,n}/k_{2,i+1,n}$, in Eq. *9* was set at unity. This assumption leads to apparent subsite binding-affinities, $\Delta\tilde{G}_i$, containing both thermodynamic and kinetic parameters. It is now shown how these apparent $\Delta\tilde{G}_i$ values may be corrected for the contribution of the kinetic ratio.

Eq. *9* shows that the bond-cleavage ratio for a pair of adjacent bonds on a substrate of chain length n measures the apparent difference in monomer binding-affinities for two subsites separated by $n-1$ subsites. For example, consider binding modes VII, 3 and VIII,3 of Fig. 1. The ratio [×]/[○–×] gives the apparent difference in binding affinity of subsites V and VIII. The apparent difference in binding affinities of other pairs of subsites can be obtained by using substrates of different chain-lengths. As bond-cleavage frequencies generate only apparent binding-affinities, it is convenient to select one subsite as a reference subsite, set $\Delta\tilde{G}_{ref} = 0$, and compare $\Delta\tilde{G}_i$ to $\Delta\tilde{G}_{ref}$.

Fig. 2 (open bars) shows the results of this comparison for BLA-N when subsite IX was chosen as the reference subsite. The salient feature of this Figure is that the $\Delta\tilde{G}_i$ value for a series of subsites on both ends of the mapped region of the enzyme appear to be constant at 1100 ± 150 cal mole^{-1}. These peripheral subsites having a constant apparent free-energy are virtual subsites or regions in space occupeid by monomer residues that are not actually a part of the enzyme-specificity site. These virtual subsites therefore delimit the real subsites (points of contact) which comprise the specificity region of the enzyme that interacts with substrate monomer-units.

*Liquefying alpha amylase from *Bacillus amyloliquefaciens*, (1→4)-α-D-glucan 4-glucanohydrolase [EC 3.2.1.1]. The following notations, introduced by Iwasa *et al.*[23], are used to distinguish the three amylases: BLA-N, (Nagase Sangyo Co., Ltd.) studied by Thoma *et al.*[17,18]; BLA-F (Fukumoto) and BLA-D (Daiwa Kasei Co., Ltd.) studied by Iwasa *et al.*[23].

Bond-cleavage frequencies then measure the number of subsites and the position of the catalytic site. Later, it will be shown how these relative $\Delta\tilde{G}_i$ values are transformed to an absolute scale.

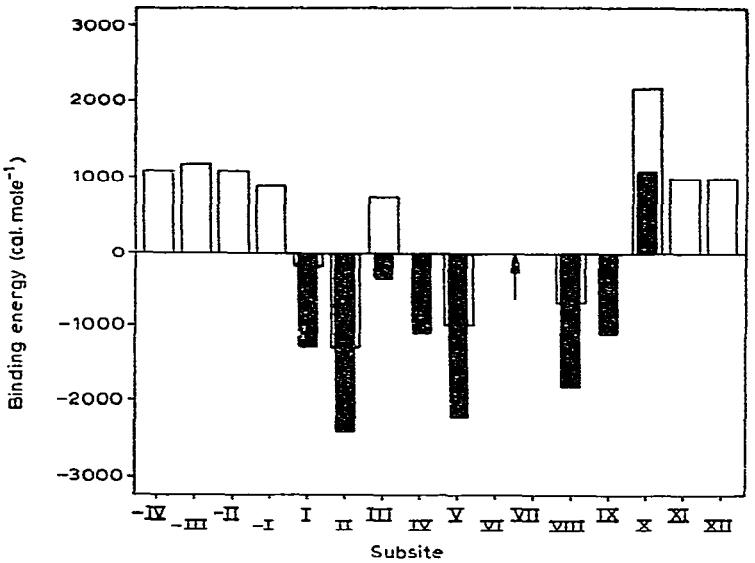

Fig. 2. Subsite binding-energies for BLA-N obtained from quantitative bond-cleavage frequency analysis[17]: ↑, position of catalytic site; □, apparent binding-energies relative to sibsite IX. The term $\Delta\tilde{G}_{IX}$ was arbitrarily set to zero and used as a reference subsite. ■, apparent binding energies obtained by correcting subsites −IV through −I, XI, and XII, (which lie beyond the end of the binding region) to zero. These apparent binding-energies contain a kinetic term (Eq. *9*). Subsites VI and VII cannot be estimated from bond-cleavage frequencies.

Iwasa and coworkers[23] used the chain-length dependence of $\tilde{V}$ (Eq. *6*) to measure the number of subsites and used qualitative bond-cleavage frequencies to locate the position of the catalytic site. Their analysis rests on the assumption that a plot of log $\tilde{V}$ *vs.* chain length, n, will exhibit a sharp break when the chain length of the substrate equals the number of subsites. A close inspection of Eq. *6* reveals that log $\tilde{V}$ *vs.* n will plateau whenever productive complexes dominate nonproductive complexes. Frequently, the concentration of productive complexes will become dominant when the chain length of the substrate is shorter than the size of the binding region. This is particularly apt to happen when a steric impediment to binding occurs near one end of the specificity site. These barrier sites are almost certainly present on all exoenzymes. Consequently, the break in a plot of log V *vs.* n will only set lower bounds on the number of interacting subsites.

The data gathered for three strains of *B. amyloliquefaciens*, BLA-N, -D and -F illustrate this point. Fig. 3 is a plot of log $\tilde{V}$ *vs.* chain length for these three enzymes. The breaks in the curves occur approximately at a chain length of eight or nine residues. However, the bond-cleavage frequency analysis for $n = 3$–12 (Fig. 2)

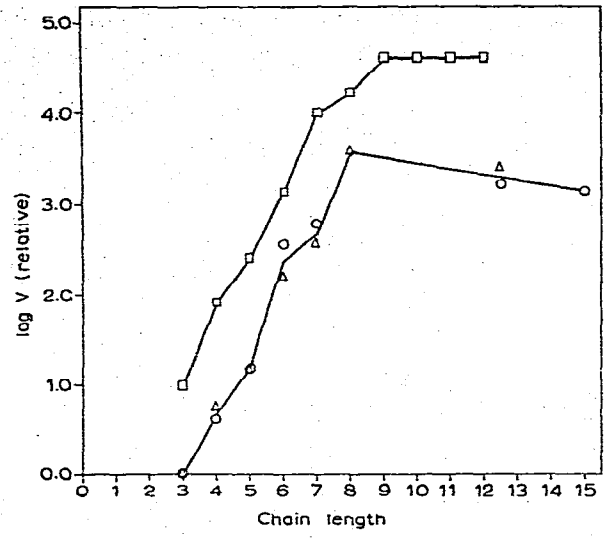

Fig. 3. Experimental dependence of $\tilde{V}$ on chain length for three strains of *B. amyloliquefaciens* amylase, BLA-N, -D and -F: ○, BLA-F; △, BLA-D, data of Iwasa *et al.*[23]; □, BLA-N data of Thoma *et al.*[18]. Data are normalized to V_3. The data for BLA-N have been displaced +1 log unit for clarity of presentation.

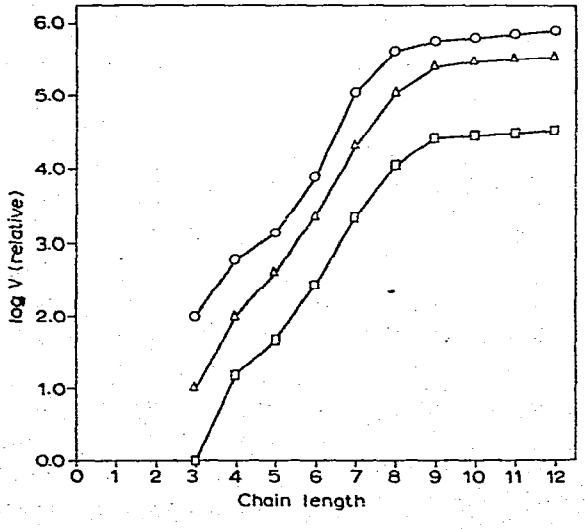

Fig. 4. Computed dependence of $\tilde{V}$ on chain length: The $\Delta\tilde{G}_t$ values of Fig. 6 (closed bars) for BLA-N were used as a basis for computations. $\tilde{V}$ was calculated from Eq. 6 and normalized to $\tilde{V}_3$. □, ten-subsite enzyme using complete energy-histogram for BLA-N; △, hypothetical nine-subsite enzyme generated by assigning $\Delta\tilde{G}_X = 0$; and ○, hypothetical eight-subsite enzyme, generated by assigning $\Delta\tilde{G}_{IX} = \Delta\tilde{G}_X = 0$. Data for the hypothetical nine- and eight-subsite enzymes are displaced +1 and +2 log units respectively for clarity of presentation.

requires that BLA-N has ten, and not eight or nine, subsites. An eight- or nine-subsite map is completely inadequate to account for the experimental data.

Fig. 4 displays simulated data for an eight-, nine-, and ten-subsite enzyme and confirms our suggestion that the break in a plot of log $\tilde{V}$ *vs.* n only sets a lower limit on the size of the binding region. The $\tilde{V}$ values for a ten-subsite map were calculated from Eq. *6* by using the subsite binding-energies for BLA-N (Fig. 2). For the hypothetical nine-subsite enzyme, ΔG_X was set at zero; for the hypothetical eight-subsite enzyme, ΔG_X and ΔG_{IX} were set at zero. For the ten-subsite enzyme, the break in the curve appears to occur at a chain length of nine, which again underestimates the true size of the binding region. The problem of determining the position of the break in the curve becomes considerably more difficult with real data because of experimental scatter.

To predict the position of the catalytic site, Iwasa and coworkers[23] have relied on qualitative bond-cleavage patterns from end-labeled oligosaccharides for one enzyme (BLA-F) and from unlabeled oligosaccharides for another (BLA-D). They conclude, using oligosaccharides of chain lengths 3–8, that the bond-cleavage frequencies were more consistent with an eight- rather than a nine- or ten-subsite enzyme. The hazards of using qualitative product-ratios to predict the number of subsites are demonstrated in Fig. 5. It is apparent that, for substrates of size equal to or smaller than the length of the binding region (Fig. 5A–B), the bond-cleavage

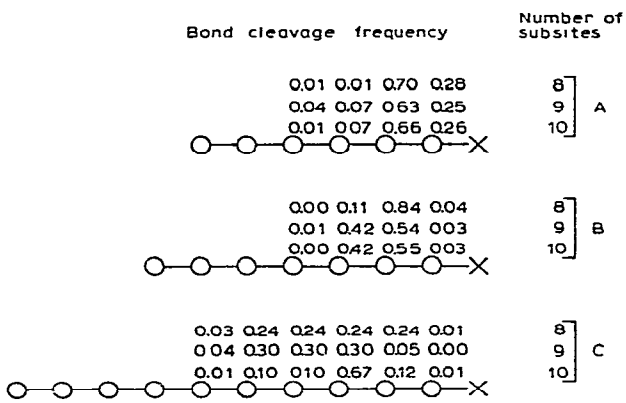

Fig. 5. Computed bond-cleavage frequencies of end-labeled oligosaccharides: ○, D-glucopyranoside residue; ×, radiolabeled D-glucopyranoside residue; ——, α-(1→4) bond. The bond-cleavage frequencies were computed for Eq. *8* for: A, maltoneptaose: B, maltooctaose; and C, maltoundecaose. For a ten-subsite enzyme, the binding energies for BLA-N in Fig. 6 (closed bars) were used; for a hypothetical nine-subsite enzyme $\Delta\tilde{G}_X = 0$; and for a hypothetical eight-subsite enzyme $\Delta\tilde{G}_X = \Delta\tilde{G}_{IX} = 0$.

frequencies show little dependence on the number of subsites. We must conclude that the qualitative bond-cleavage patterns reported by Iwasa *et al.*[23] are consistent with an enzyme containing eight, nine, or ten subsites and, therefore cannot differentiate between the three possibilities. It is only when the chain length exceeds the length of

the specificity region that bond-cleavage frequencies depend markedly on the size of the specificity region (Fig. 5C). These long substrates are excellent probes of the length of the binding region.

The use of unlabeled substrates further complicates the problem of locating the catalytic site, because two positional isomers will yield identical products upon hydrolysis. For example, hydrolysis of the two productive complexes of maltotriose (Fig. 1) both yield the same products, namely D-glucose and maltose. It is impossible to tell what fraction of D-glucose arose from cleavage at the reducing end of the molecule and what fraction arose from cleavage at the nonreducing end. Consequently it is impossible to distinguish a real subsite-map from its "mirror image". However, if the maltotriose is radiolabeled at the reducing end, the production of labeled D-glucose and labeled maltose unambigously pinpoints the relative rate of hydrolysis of the two bonds (see Fig. 1).

Determination of subsite binding-affinities. — A brief account of the techniques designed to estimate monomer subsite binding-affinities, $\Delta\bar{G}_i$, from experimental data is now discussed. Iwasa *et al.*[23] did not quote our 1971 paper[17] where it was shown that both bond-cleavage frequencies and Michaelis parameters are required to generate a *complete* subsite map. They then claimed that our bond-cleavage frequency

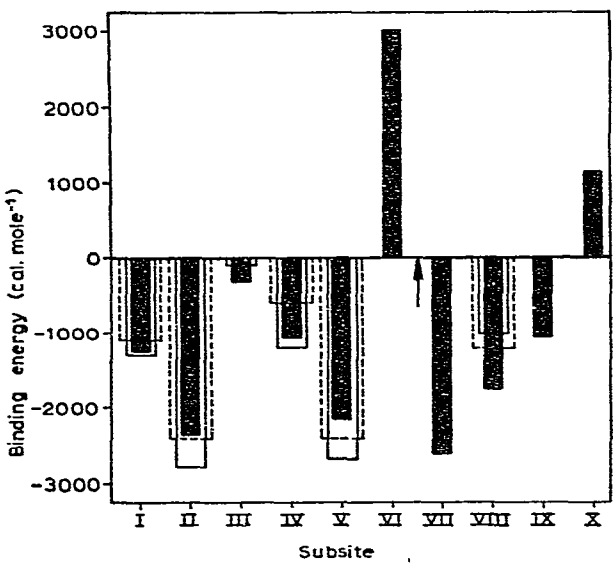

Fig. 6. Comparison of subsite maps for three strains of *B. amyloliquefaciens:* ■, BLA-N computed by model of Thoma *et al.*[17,18]; □, BLA-D, ⬚, BLA-F predicted by Iwasa *et al.*[23]. For BLA-N, binding energies for subsites I–V and VIII–X were determined from bond-cleavage frequency analysis[17] and binding energies for subsites VI and VII were estimated from Michaelis parameters[18]. For BLA-D and BLA-F, binding energies for subsites I–V and VIII were estimated from initial-velocity ratios[23]. For BLA-D and BLA-F, the sum of the binding energies for subsites VI and VII was estimated to be 3800 and 3100 cal. mole^{-1} respectively[23]; this sum was not divided between the two subsites.

analysis (1970 paper)[18] and their thermodynamic analysis are complementary, and that they appear to generate a similar subsite map (Fig. 6). However, the visual similarities of subsite-energy histograms are deceiving because the chain-length dependence of $\tilde{K}_m$, $\tilde{V}$, and bond-cleavage frequencies are very sensitive to $\Delta\tilde{G}_i$ values. Consequently, the procedure used to generate subsite-energy histograms is of the utmost importance.

The procedure devised by Iwasa *et al.*[23] to calculate ΔG_i for BLA-D and BLA-F relies on measured first-order rate constants (Eq. 7). By dividing $\tilde{v}_{0,n}$ by $\tilde{v}_{0,2}$, they obtained the general equation:

$$\frac{\tilde{v}_{0,n}}{\tilde{v}_{0,2}} = \frac{\sum_t k_{2,t,n} \exp(-\sum_i \Delta\tilde{G}_i/RT)}{\sum_t k_{2,t,2} \exp(-\sum_i \Delta\tilde{G}_i/RT)}. \qquad (10)$$

They then simplified Eq. *10* by making the assumption that k_2 is an intrinsic constant. For example, when $n = 3$, Eq. *10* becomes

$$\frac{\tilde{v}_{0,3}}{\tilde{v}_{0,2}} = \exp(\Delta\tilde{G}_V + \Delta\tilde{G}_{VIII})/RT. \qquad (11)$$

For different values of n they obtained a series of nonlinear equations of the form of Eq. *11*. They then attempted an iterative technique to solve this set of nonlinear equations (see Appendix for details). As noted before, these equations do not supply any information about the two subsites adjacent to the catalytic site. Iwasa *et al.*[23] calculated the sum of the binding energies of these two subsites (subsites VI and VII) adjacent to the catalytic site from $\tilde{v}_{0,2}$ and an independent estimate for k, but they could not proportion the sum between these two subsites. Fig. 6 shows the partial subsite-maps generated for BLA-D and BLA-F by this technique.

This procedure, although theoretically sound if k_2 is an intrinsic constant, (discussed later) suffers from several practical pitfalls. First, division of $\tilde{v}_{0,n}$ by $\tilde{v}_{0,2}$ propagates any error in measurement of the latter value throughout the entire set of equations (Eq. *11*). As $\tilde{v}_{0,n}$ decreases by 5 or 6 orders of magnitude as n changes from 8 to 2, trace contamination of a maltase could seriously raise $\tilde{v}_{0,2}$ above its real value. A second practical problem is the instability of the series of nonlinear, simultaneous equations (Eq. *11*). We have found that Iwasa and coworkers'[23] iterative technique for solving this set of equations does not always converge to a unique solution. Oscillations sometimes tend to amplify themsleves on succession iterations, and this leads to divergence. The amplification factor is extremely sensitive to measured $\tilde{v}_{0,n}$ values (see Appendix for details).

The procedure proposed by our group[17,18] for evaluating the subsite binding-energies is based on the combined use of Eqs. *5*, *6*, and *8*. The analysis is begun by using quantitative bond-cleavage frequencies to generate the relative subsite-map shown in Fig. 2 (open bars). As noted before, subsites −IV through −I, XI, and XII lie beyond the edge of the binding region; hence, their absolute binding-affinity for a

substrate monomer unit must be zero. These subsites have a $\Delta\tilde{G}$ value of 1100 $\pm$150 cal.mole^{-1} relative to subsite IX (the reference subsite). By lowering $\Delta\tilde{G}_i$ for each subsite by 1100 cal.mole^{-1}, the subsite energy histogram is transformed to an absolute scale, as shown in Fig. 2 (closed bars).

Bond-cleavage frequencies (Eq. *9*), like $\tilde{v}_{0,n}/\tilde{v}_{0,2}$ ratios (Eq. *7*), only sense productive complexes and cannot furnish any information about the subsites (VI and VII) adjacent to the catalytic site. However, $\tilde{K}_m$ and $\tilde{V}$ contain information about both productive and nonproductive complexes, and they must be used to predict the energies of the two subsites adjacent to the catalytic site.

We used a weighted, least-squares analysis to calculate $\Delta\tilde{G}_{VI}$ and $\Delta\tilde{G}_{VII}$ for BLA-N[18]. First, the sum of the binding energies of these two subsites was measured, and then the sum was proportioned between the two subsites in a way that optimizes the fit between computed and experimental $\tilde{K}_m$ and $\tilde{V}$ values. The sum of $\Delta\tilde{G}_{VI}$ and $\Delta\tilde{G}_{VII}$ was computed from the equation:

$$\Delta\tilde{G}_{VI}+\Delta\tilde{G}_{VII} = -RT\ln K_{int}+2400-\sum_i \Delta\tilde{G}_i, \qquad (12)$$

$$(i \neq \text{VI or VII})$$

where $\Delta\tilde{G}_i$ values ($i \neq$ VI or VII) were obtained from bond-cleavage frequencies (Fig. 2, closed bars). K_{int}, the association constant for internal binding, is the microscopic association-constant for an enzyme–substrate complex where the active site is completely filled. K_{int} can be evaluated from $\tilde{K}_{m,n}$ for substrates having a chain length equal to, or greater than, the size of the binding region.

The subsite map generated for BLA-N by this technique was then tested for its ability to reproduce $\tilde{K}_m$ and $\tilde{V}$ as a function of chain length ($n = 3$–8). The resulting residual error exceeded the experimental error by an order of magnitude. We were then forced to conclude that the subsite model, as originally conceived, required modification[18]. It was concluded, from trends in experimental data, that ignoring the contribution of $k_{2,i,n}/k_{2,i+1,n}$ to $\Delta\tilde{G}_i$ values (Eq. *9*) caused the relative subsite binding-affinities to be overestimated.

As a specific example, the hydrolysis of maltooctaose bound in modes VII,8 and VIII,8 (Fig. 1) is now considered. Rearranging terms in Eq. *9* gives

$$\Delta G_{VIII} = RT\ln\frac{[\times]}{[\bigcirc-\times]} + RT\ln\frac{k_{2,VIII,8}}{k_{2,VII,8}}, \qquad (13)$$

so that the binding affinities of Fig. 2 (closed bars) must be corrected by the factor $RT\ln(k_{2,VIII,8}/k_{2,VII,8})$. The experimental data indicate that, *to a first approximation*, the filling of any subsite lowered the activation-energy barrier by a relatively constant amount. This observation may be expressed mathematically as

$$k_{2,i,n} \propto \exp\left(\sum_i \Delta G_{a,i}/RT\right), \qquad (14)$$

where $\Delta G_{a,i}$ is the contribution of the ith subsite to the acceleration of bond cleavage.

Substitution of Eq. *14* into Eq. *13* yields

$$\Delta G_{\text{VIII}} = RT \ln \frac{[\times]}{[\bigcirc\!-\!\times]} + \Delta G_{a,\text{VIII}}. \qquad (15)$$

Therefore, the subsite binding-energies obtained from bond-cleavage frequencies must be increased by the factor $\Delta G_{a,i}$. Because we cannot evaluate $\Delta G_{a,i}$ individually, we were forced, as a first approximation, to use an average value for the acceleration factor. When the subsite binding-energies were corrected for this average acceleration term (which amounted to 450 cal.mole^{-1}), the resulting subsite map sucessfully predicted the experimental parameters within the experimental error. The final subsite map for BLA-N is shown in Fig. 6. It is not implied that ΔG_a is a constant, but only that assigning it some mean value dramatically improves the predictive value of the model.

Iwasa and coworkers[23], in constrast, have maintained that ΔG_a cancels from Eqs. *8* and *13–15*. They have rejected the possibility that k_2 is a function of the number of filled subsites because it "is *a priori* unlikely" and have stated that the assumption that k_2 is an intrinsic constant is essential as a working hypothesis. It must be emphasized that our position that k_2 is an *average* function of the number of occupied subsites was an alteration of the subsite model dictated by experimental data. Only by relaxating the restraint that k_2 is an intrinsic constant could we modify the model to bring experimental and computed parameters into agreement. This modification of the model was a matter of *a posteriori* reasoning and not *a priori* speculation.

Iwasa and coworkers[23] claim that the constancy of k_2 has been demonstrated with an exoamylase, glucoamylase. Hiromi *et al.*[21] obtained good agreement between experimental and calculated Michaelis parameters for glucoamylase by assuming that k_2 was a constant. This seems to indicate that ΔG_a is negligible for glucoamylase but is not sufficient evidence to summarily reject the possibility of a contribution from ΔG_a for other enzymes. In fact, it will be shown that the experimental data of Iwasa and coworkers[23] for BLA-D amylase indicates that k_2 is a variable.

Iwasa and coworkers have computed subsite binding-energies with the aid of Eq. *8*. The free energies for filling subsites computed by this procedure are similar to those computed from bond-cleavage frequencies in that the apparent ΔG values contain a rate ratio, $k_{2,i,n}/k_{2,i,n+1}$. To take a specific example, when $n=3$, Eq. *10* becomes

$$\frac{\tilde{v}_{0,3}}{\tilde{v}_{0,2}} = \frac{k_{2,\text{VIII},3}}{k_{2,\text{VII},2}} \exp(-\Delta G_{\text{VIII}}/RT) + \frac{k_{2,\text{VII},3}}{k_{2,\text{VII},2}} \exp(-\Delta G_{\text{V}}/RT). \qquad (16)$$

Substituting Eq. *14* into Eq. *16* and solving for the free energy associated with subsite V yields an expression similar to Eq. *15*, namely

$$\Delta \tilde{G}_{\text{V}} - \Delta \tilde{G}_{a,\text{V}} = -RT \ln \frac{\tilde{v}_{0,3}}{\tilde{v}_{0,2}} \exp(\Delta G_{a,\text{VIII}} - \Delta G_{\text{VIII}})/RT. \qquad (17)$$

Hence the true subsite binding-energies are equal to those calculated by Iwasa and coworkers[23] plus $\Delta G_{a,i}$, the acceleration factor.

As Iwasa and coworkers[23] have not evaluated the individual binding-energy of the two subsites adjacent to the catalytic site, they lack a crucial data set needed to compute the chain-length dependence of $\tilde{K}_m$ and $\tilde{V}$. This lack of data prevents them from comparing computed and experimental Michaelis constants to check on the merits of their model. We therefore used our statistical minimization-technique[18] and the $\tilde{K}_m$ and $\tilde{V}$ data of Iwasa and coworkers[23] to optimize $\Delta\tilde{G}_{VI}$ and $\Delta\tilde{G}_{VII}$ for BLA-D, setting $\Delta G_a = 0$. A comparison of the computed and experimental parameters is made in Table II. On the average, the computed values differ from the experimental values by two orders of magnitude. However, if the constraint that k_2 is a constant is relaxed and ΔG_a is optimized, a dramatic improvement in fit results (Table II).

TABLE II

EFFECT OF ACCELERATION FACTOR ON BLA-D AMYLASE[a]

Chain length	*Experimental*[b] $\tilde{K}_m$ (M)	*Experimental* $\tilde{K}_m$ / *Calc* $\tilde{K}_m$		*Experimental*[b] $\tilde{V}$ (*relative*)	*Experimental* $\tilde{V}$ / *Calc* $\tilde{V}$	
		$\Delta G_a = 0$	$\Delta G_a = 630$		$\Delta G_a = 0$	$\Delta G_a = 630$
3	1.7×10^{-1}	12	3.5	1.0	*c*	*c*
4	3.3×10^{-2}	62	1.8	5.7	12	1.2
5	3.5×10^{-2}	530	3.9	1.6×10	66	1.7
6	1.6×10^{-2}	244	3.6	1.6×10^{2}	32	1.7
7	1.3×10^{-2}	201	8.4	3.8×10^{2}	5.9	0.9
8	3.8×10^{-3}	61	4.8	3.6×10^{3}	13	3.7

[a] $\tilde{K}_m$ and $\tilde{V}$ were calculated by using the subsite binding-energies estimated from initial velocity by Iwasa *et al.*[23], except for subsites VI and VII, which were optimized to give the best fit with k_2 constant ($\Delta G_a = 0$) or with an acceleration factor ($\Delta G_a = 630$ cal/mole). The optimized binding-energies for subsites VI and VII are 2670 and -3650 cal mole^{-1}, respectively. [b] The experimental values were measured for malto-oligosaccharides by Iwasa *et al.*[23]. [c] Velocities for maltotriose were used to normalize that $\tilde{V}$ values, so that by definition, experimental $\tilde{V}_3$/calc. $\tilde{V}_3 = 1$.

It is proposed that this improvement in the model supports our belief that the enzyme utilizes a portion of the free energy released upon substrate binding to lower the activation-energy barrier for hydrolysis. Substrate binding is therefore an integral part of catalysis and not, as the analysis by Iwasa *et al.* insists, merely a process that preceeds catalysis. We do not imply that 630 cal.mole^{-1} in Table II is the correct value of ΔG_a for BLA-D because of the uncertainty of the number of subsites and the position of the catalytic site. The best way to resolve these contested points is by careful, quantitative bond-cleavage frequency-analyses of end-labeled substrates.

CONCLUSIONS

This comparative study reveals that the thermodynamic and kinetic behavior of depolymerizing enzymes is sensitive to small variations in subsite binding-energies.

Hence, conclusions concerning the similarities of enzymes, based upon visual comparisons of subsite maps may be misleading (Fig. 6). The value of any theoretical model lies in its ability to account for experimental facts and in its ability to make correct predictions. For this reason, it is imperative that any subsite map generated by the complex manipulation of experimental data be tested for its ability to reproduce the original experimental data before it is accepted.

As the subsite map of Iwasa and coworkers[23] for BLA-D does not satisfactorily account for their data, we believe it must be modified or rejected. The inadequacy of their model is traced partly to inadequate data collection and difficulties in data processing and partly to their insistence that k_2 is an intrinsic constant[19–25]. Because of the complexity of the subsite model, the computed number of subsites and subsite binding-energies critically depends upon data-processing techniques. For example, the number of subsites derived from an analysis of the chain-length dependence of bond-cleavage frequencies will generally exceed the number of subsites derived from an analysis of the chain-length dependence of Michaelis parameters. Any technique that incorrectly counts the number of binding modules inevitably generates an erroneous subsite map.

Because of its successful application, we believe that the bond-cleavage frequencies method[17] is the best way to determine the number of binding modules and to locate the catalytic site. The advantage of measuring bond-cleavage frequencies is that a single series of experiments determines the size of the binding region, the position of the catalytic site, and the relative binding-energies of all subsites except those adjacent to the catalytic site. A deficiency of using only this information as well as Hiromi's approach is that they both introduce contributions from kinetic terms (the acceleration factor) into the apparent binding-energies. Michaelis parameters are required to sort the apparent binding-energies into the kinetic and the thermodynamic components.

When the experimental data forced us to abandon the assumption that k_2 was constant, that assumption was replaced with the approximation that, *on the average*, for *B. amyloliquefaciens* amylase (BLA-N), filling a module increased k_2 roughly by a factor of two. At present there is no way to evaluate ΔG_a associated with a given, productive positional isomer, and an average value for ΔG_a can only be estimated. This problem of ΔG_a will need to be handled on an *ad hoc* basis for each new enzyme investigated until generalities begin to emerge.

In conclusion, to map the specificity site of an enzyme requires *two* types of input, quantitative bond-cleavage frequencies as a function of chain length *and* Michaelis parameters ($\tilde{K}_m$ and $\tilde{V}$) as a function of chain length. Either type of data alone will give an incomplete, and possibly erroneous, subsite map. The following steps are recommended for subsite mapping:

1. Establish experimental conditions where complicating factors such as bimolecular reactions[16] and multiple attack are insignificant[20] or modify the model to account for these factors.

2. Use end-labeled substrates to determine quantitative bond-cleavage

TABLE III

A COMPARISON OF SYMBOLS AND NOTATIONS USED BY TWO RESEARCH GROUPS FOR SUBSITE MAPPING[a]

Symbols of Thoma et al.[17,18]	*Symbols of Iwasa* et al.[23]	*Definition*
Symbols		
A		Substrate
	A	Subsite affinity
	b	Molecular activity, k_0, divided by the Michaelis constant
E	E	Enzyme
	e_0	Enzyme concentration
ΔG	ΔG	Standard free-energy
k	k	Unimolecular or bimolecular rate-coefficient
	k_0	Molecular activity, the maximum velocity divided by the molar concentration of enzyme
K	K	Microscopic or macroscopic equilibrium-constant
K_m	K_m	Michaelis constant
P		Product
	P	Probability of cleavage
R	R	Gas constant
	S	Substrate
	s	Substrate concentration
T	T	Absolute temperature
v_0	v	Initial velocity at $A << \tilde{K}_m$
V	V	Maximum velocity
[ ]	[ ]	Concentration
	cov.	Subsites "covered" or occupied by substrate monomer units.
Subscripts		
a		Acceleration factor
i	i, r	Subsite index
int		Property of a chain completely occupying the binding region
	int	"Intrinsic" rate coefficient for hydrolysis
ι	j	Binding-mode index, subsite number occupied by the "reducing" D-glucosyl residue
m		Chain length of product
n		Chain length of substrate
	p	Binding-mode index for productive binding
1		Microscopic, bimolecular dissociation-coefficient
-1		Microscopic, unimolecular dissociation-coefficient
2		Microscopic, unimolecular rate-coefficient
0		Initial or total quality
Superscripts		
$\sim$		Measured or apparent value
′		Association constant
·		Time derivative

[a]For additional notations, see Ref. 18.

frequencies and establish the size of specificity site, the position of the catalytic amino acids, and the apparent binding-energies of the subsites.

3. Measure $\tilde{K}_m$ and $\tilde{V}$ as a function of chain length.

4. Utilize optimization* techniques to establish the binding energy of the two sites adjacent to the catalytic site and estimate ΔG_a.

5. Test the resulting model-parameters for their ability to reproduce the experimental data.

6. Modify the model if necessary, recompute new set of model parameters, and recheck the ability of these parameters to reproduce the experimental data.

APPENDIX

Evaluation of subsite affinities from initial-velocity measurements. — As outlined in the text, Iwasa *et al.*[23] used initial-velocity ratios to estimate subsite binding-energies, ΔG_i. The general equation is

$$\frac{\tilde{v}_{0,n}}{\tilde{v}_{0,2}} = \frac{\sum_i k_{2,i,n} \exp(-\sum \Delta G_i/RT)}{\sum_i k_{2,i,2} \exp(-\sum \Delta G_i/RT)}, \qquad (A1)$$

where $\tilde{v}_{0,n}$ is the first-order rate constant measured at $A \ll K_m$.

These authors assumed that k_2 is constant and that the rate terms cancel from Eq. *A1*. For BLA-D or -F, the following series of equations are generated for $n = 3$–8:

$$\frac{\tilde{v}_{0,3}}{\tilde{v}_{0,2}} = \exp(-\Delta G_V/RT) + \exp(-\Delta G_{VIII}/RT), \qquad (A2)$$

$$\frac{\tilde{v}_{0,4}}{\tilde{v}_{0,2}} = \exp\{(-\Delta G_{IV} - \Delta G_V)/RT\} + \exp\{(-\Delta G_V - \Delta G_{VIII})/RT\} + \exp(-\Delta G_{VIII}/RT), \qquad (A3)$$

$$\frac{\tilde{v}_{0,5}}{\tilde{v}_{0,2}} = \exp\{(-\Delta G_{III} - \Delta G_{IV} - \Delta G_V)/RT\} + \exp\}(-\Delta G_{IV} - \Delta G_V - \Delta G_{VIII})/RT\} + \exp\{(-\Delta G_V = \Delta G_{VIII})/RT\} + \exp\{-\Delta G_{VIII}/RT\}, \qquad (A4)$$

$$\frac{\tilde{v}_{0,6}}{\tilde{v}_{0,2}} = \exp\{(-\Delta G_{II} - \Delta G_{III} - \Delta G_{IV} - \Delta G_V)/RT\} + \exp\{(-\Delta G_{III} - \Delta G_{IV} - \Delta G_V - \Delta G_{VIII})/RT\} + \exp\{(-\Delta G_{IV} - \Delta G_V - \Delta G_{VIII})/RT\} + \exp\{(-\Delta G_V - \Delta G_{VIII})/RT\} + \exp\{-\Delta G_{VIII}/RT\}, \qquad (A5)$$

*Minimization programs are available upon request.

$$\frac{\tilde{v}_{0,7}}{\tilde{v}_{0,2}} = \exp\{(-\Delta G_{\mathrm{I}}-\Delta G_{\mathrm{II}}-\Delta G_{\mathrm{III}}-\Delta G_{\mathrm{IV}}-\Delta G_{\mathrm{V}})/RT\}+$$
$$+\exp\{(-\Delta G_{\mathrm{II}}-\Delta G_{\mathrm{III}}-\Delta G_{\mathrm{IV}}-\Delta G_{\mathrm{V}}-\Delta G_{\mathrm{VIII}})/RT\}+$$
$$+\exp\{(-\Delta G_{\mathrm{III}}-\Delta G_{\mathrm{IV}}-\Delta G_{\mathrm{V}}-\Delta G_{\mathrm{VIII}})/RT\}+$$
$$+\exp\{(-\Delta G_{\mathrm{IV}}-\Delta G_{\mathrm{V}}-\Delta G_{\mathrm{VIII}})/RT\}+$$
$$+\exp\{(-\Delta G_{\mathrm{V}}-\Delta G_{\mathrm{VIII}})/RT\}+\exp\{-\Delta G_{\mathrm{VIII}}/RT\}, \qquad (A6)$$

and

$$\frac{\tilde{v}_{0,8}}{\tilde{v}_{0,2}} = \exp\{(-\Delta G_{\mathrm{I}}-\Delta G_{\mathrm{II}}-\Delta G_{\mathrm{III}}-\Delta G_{\mathrm{IV}}-\Delta G_{\mathrm{V}})/RT\}+$$
$$+\exp\{(-\Delta G_{\mathrm{I}}-\Delta G_{\mathrm{II}}-\Delta G_{\mathrm{III}}-\Delta G_{\mathrm{IV}}-\Delta G_{\mathrm{VIII}})/RT\}+$$
$$+\exp\{(-\Delta G_{\mathrm{II}}-\Delta G_{\mathrm{III}}-\Delta G_{\mathrm{IV}}-\Delta G_{\mathrm{V}}-\Delta G_{\mathrm{VIII}})/RT\}+$$
$$+\exp\{(-\Delta G_{\mathrm{III}}-\Delta G_{\mathrm{IV}}-\Delta G_{\mathrm{V}}-\Delta G_{\mathrm{VIII}})/RT\}+$$
$$+\exp\{(-\Delta G_{\mathrm{IV}}-\Delta G_{\mathrm{V}}-\Delta G_{\mathrm{VIII}})/RT)\}+$$
$$+\exp\{(-\Delta G_{\mathrm{V}}-\Delta G_{\mathrm{VIII}})/RT\}+\exp\{-\Delta G_{\mathrm{VIII}}/RT\}. \qquad (A7)$$

Iwasa and his coworkers[23] proposed to solve this set of simultaneous, nonlinear equations by the following iterative technique: 1. Select a starting value for ΔG_{VIII}. 2. With this initial guess, calculate ΔG_{V} from Eq. *A2*. 3. Substitute these values of ΔG_{VIII} and ΔG_{V} into Eq. *A3* and solve for ΔG_{IV}. 4. Continue in this manner until a new value for ΔG_{VIII} is found from Eq. *A7*. 5. Substitute the new value of ΔG_{VIII} into Eq. *A3* and repeat steps 2–5 until "self-consistent values of ΔG_i values are obtained" (converge to a solution).

We found that, when the subsite binding-energies reported for BLA-F were substituted in Eqs. *A2-A7*, we could not regenerate the experimental values of $\tilde{v}_{0,n}/\tilde{v}_{0,2}$. Although the iterative procedure designed to solve Eqs. *A2–A7* is theoretically sound, we have found that the equations are unstable and that the iterative technique leads to divergence rather than covergence. For BLA-D, iteration did lead to convergence; however, for BLA-F, iteration caused divergence. Iwasa *et al.* reported that convergence was obtained when $\Delta G_{\mathrm{VIII}} = 1200$ cal.mole^{-1} for BLA-F. If this value is used as an initial guess in Eq. *A2*, the second iteration fails because the logarithm of a negative number is encountered in Eq. *A5*. Fig. 7 demonstrates the instability of these equations.

In a subsequent paper, this same research group examined the effect of photooxidation on BLA-D[24]. They found that $\tilde{v}_{0,n}$ ($n = 3$–12.6) was depressed by 20–90%. We attempted to generate a subsite map for this modified BLA-D by using Eqs. *A2–A8*. As $\tilde{v}_{0,2}$ for the modified BLA-D was not given, we assumed that, it was depressed by the same amount as $\tilde{v}_{0,3}$ and $\tilde{v}_{0,4}$. Even by choosing a wide range of initial values for ΔG_{VIII}, we were not able to obtain convergence.

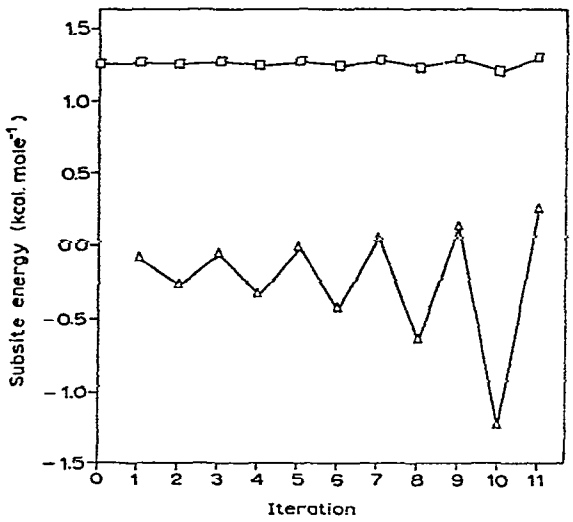

Fig. 7. Oscillations in the $\Delta\tilde{G}_i$ values for BLA-F with successive iterations, by using Eq. *A2–A7* and the experimental data of Iwasa *et al.*[23]: □, $\Delta\tilde{G}_{VIII}$; △, $\Delta\tilde{G}_{II}$. The initial value of $\Delta\tilde{G}_{VIII}$ was 1.26 kcal. mole^{-1}. Iwasa *et al.* reported convergence at $\Delta\tilde{G}_{VIII} = 1.2$ kcal. mole^{-1}.

Eqs. *A2–A7* are even more complex if the enzyme has another subsite to the right of the catalytic site. In this situation, Eq. *A2* now has terms for ΔG_V, ΔG_{VIII}, and ΔG_{IX}, so that an initial guess would have to be made for two subsites, compounding the problem of obtaining a solution.

ACKNOWLEDGMENTS

This research was supported in part by Agricultural Research Service, U.S. Department of Agriculture, Grant 12-14-100-9908(71), administered by the Northern Regional Research Laboratory, and by National Science Foundation Grant BMS-74-19838. Computing services were supported by a University of Arkansas Computing Grant.

REFERENCES

1 I. SCHECHTER AND A. BERGER, *Biochem. Biophys. Res. Commun.*, 27 (1967) 157–162.
2 N. ABRAMOWITZ, I. SCHECHTER, AND A. BERGER, *Biochem. Biophys. Res. Commun.*, 29 (1967) 862–867.
3 K. MORIHARI AND T. OKA, *Biochem. Biophys. Res. Commun.*, 30 (1968) 625–630.
4 K. MORIHARA, T. OKA, AND H. TSUZUKI, *Biochem. Biophys. Res. Commun.*, 35 (1969) 210–214.
5 D. ATLAS, S. LEVIT, I. SCHECHTER, AND A. BERGER, *FEBS Lett.*, 11 (1970) 281–283.
6 R. C. THOMPSON AND E. R. BLOUT, *Proc. Natl. Acad. Sci. U. S. A.*, 67 (1970) 1734–1740.
7 J. R. COGGINS, W. KRAY, AND E. SHAW, *Biochem. J.*, 137 (1974) 579–585.
8 P. CUATRECUSAS, M. WILCHEK, AND C. B. ANFINSEN, *Science*, 162 (1968) 1491–1493.
9 H. M. LAZARUS, M. B. SPARN, AND D. F. BRADLEY, *Proc. Natl. Acad. Sci. U. S. A.*, 60 (1968) 1503–1510.
10 J. Y. CHOU AND M. F. SINGER, *J. Biol. Chem.*, 245 (1970) 1005–1011.
11 T. GODEFROY, *Eur. J. Biochem.*, 14 (1970) 222–231.

12 D. M. CHIPMAN, V. GRISARO, AND N. SHARON, *J. Biol. Chem.*, 242 (1967) 4388–4394.
13 D. M. CHIPMAN AND N. SHARON, *Science*, 165 (1969) 454–465.
14 E. HOLLER, J. A. RUPLEY, AND G. P. HESS, *FEBS Lett.*, 40 (1974) 25–28.
15 J. ROBYT AND D. FRENCH, *Arch. Biochem. Biophys.*, 100 (1963) 451–467.
16 J. ROBYT AND D. FRENCH, *J. Biol. Chem.*, 245 (1970) 3917–3927.
17 J. A. THOMA, C. BROTHERS, AND J. SPRADLIN, *Biochem.*, 9 (1970) 1768–1775.
18 J. A. THOMA, G. V. K. RAO, C. BROTHERS, J. SPRADLIN, AND H. L. LI, *J. Biol. Chem.*, 246 (1971) 5621–5635.
19 K. HIROMI, *Biochem. Biophys. Res. Commun.*, 40 (1970) 1–6.
20 Y. NITTA, M. MIZUSHIMA, K. HIROMI, AND S. ONO, *J. Biochem.* (Tokyo), 69 (1971) 567–576.
21 K. HIROMI, Y. NITTA, C. MUMATA, AND S. ONO, *Biochim. Biophys. Acta*, 302 (1973) 362–375.
22 M. KATO, K. HIROMI, AND Y. MORITA, *J. Biochem.* (Tokyo), 75 (1974) 563–576.
23 S. IWASA, H. AOSHIMA, K. HIROMI, AND H. HATANO, *J. Biochem.* (Tokyo), 75 (1974) 969–978.
24 H. AOSHIMA, T. MANABE, K. HIROMI, AND H. HATANO, *Biochim. Biophys. Acta*, 341 (1974) 497–504.
25 M. KATO, K. HIROMI, AND Y. MORITA, *J. Biochem.* (Tokyo), 75 (1974) 563–576.
26 T. SHIBAOKA, K. MIYAMO, AND T. WATANABE, *J. Biochem.* (Tokyo), 76 (1974) 475–479.
27 L. REXOVÁ-BENKOVÁ, *Eur. J. Biochem.*, 39 (1973) 109–115.
28 R. W. GURNEY, *Ionic Processes in Solution*, McGraw–Hill, New York, 1953, pp. 80–112.
29 K. R. HANSON, *Biochemistry*, 1 (1962) 723–734.
30 J. F. ROBYT AND D. FRENCH, *Arch. Biochem. Biophys.*, 122 (1967) 8–15.